Hindawi
Advances in Civil Engineering
Volume 2020, Article ID 8880906, 13 pages
https://doi.org/10.1155/2020/8880906

Research Article

Influence of the Nature and Rate of Alkaline Activator on the Physicochemical Properties of Fly Ash-Based Geopolymers

Marouane EL Alouani,[1] **Saliha Alehyen**,[1] **Mohammed EL Achouri**,[1] **Abdelowahed Hajjaji**,[2] **Chouaib Ennawaoui**,[2] **and M'hamed Taibi**[1]

[1]*Mohammed V University in Rabat, Centre des Sciences des Matériaux (CSM), Laboratoire de Physico-Chimie des Matériaux Inorganiques et Organiques (LPCMIO), École Normale Supérieure (ENS), Rabat, Morocco*
[2]*University Research Center on Renewable Energies & Intelligent Systems for Energy-Science Engineer Laboratory for Energy (LabSIPE), National School of Applied Sciences, Chouaïb Doukkali University, El Jadida, Morocco*

Correspondence should be addressed to Marouane EL Alouani; ma.elalouani@gmail.com

Received 13 May 2020; Revised 25 August 2020; Accepted 3 September 2020; Published 21 September 2020

Academic Editor: Francesco Colangelo

The influence of alkali cations on mix design of geopolymers is essential for their mechanical, thermal, and electrical performance. This research investigated the influence of alkali cation type on microscale characteristics and mechanical, dielectric, and thermal properties of fly ash-based geopolymer matrices. The geopolymers were elaborated via class F fly ash from the thermal plant Jorf Lasfar, El Jadida (Morocco), and several alkaline solutions. Morphological, structural, mechanical, dielectric, and thermal characteristics of materials synthesized via fly ash with different proportions of KOH and NaOH aged 28 days were evaluated. The physicochemical properties of class F fly ash-based geopolymers were assessed using X-ray diffraction (XRD), Fourier-transform infrared spectrometry (FTIR), and scanning electron microscopy coupled with energy dispersive X-ray spectroscopy (SEM/EDX) analyses. Based on readings of the results obtained, XRD and FTIR analysis detected the creation of semicrystalline potassium/sodium aluminate-silicate hydrate (KASH/NASH) gel in the elaborated matrices after the geopolymerization reaction. The SEM analysis proved the formation of alkali alumina-silicate hydrate gel in the raw material particles after the polycondensation stage. Experimental compressive strength data indicated that the highest compressive strength (39 MPa) was produced by the alkaline activator (75% KOH/25% NaOH). The dielectric parameters values of the elaborated materials changed depending of the mass ratios KOH/NaOH. Dielectric findings demonstrated that geopolymers containing 100% NaOH have better dielectric performances. The fire resistance study revealed that the geopolymer binders induced by KOH are stable up to 600°C. Based on these results, it can be deduced that the formulated geopolymer concrete possesses good mechanical, dielectric, and fire resistance properties.

1. Introduction

Nowadays, Ordinary Portland Cement (OPC) is one of the most commonly applied building materials in the world [1, 2]. The annual global production of this material has increased to 2.8 billion tons and has been estimated to increase to 4 billion tons per year in 2050 [3].

The price and availability of feedstock, the considerable demand for energy, and CO_2 emissions are significant preoccupations for the OPC industries. For example, global OPC production consumes about 12 to 15% of the world's total industrial energy consumption and the production of 1 ton of OPC generates about 0.85 to 1.1 tons of CO_2, one of the main greenhouse gases and responsible for global warming [4, 5].

The necessity to build in a sustainable, rational, and ecological way encourages innovation and the search for alternatives, such as geopolymerization technology, which is attracting increasing attention for its ability to reduce energy consumption and CO_2 emissions by approximately 60% and 80%, respectively [6–8]. The geopolymerization technology makes it possible to recover industrial wastes such as fly ash

which have a harmful impact on the environment and to develop new environmentally friendly building materials that can partially or totally replace OPC [9, 10].

Recently, many projects have been undertaken to develop geopolymer-type binders using geopolymerization technology which consume less energy and are more environmentally friendly [10–14].

The geopolymers show attractive potentials and superior properties such as fire and chemical resistances, with no CO_2 emissions during their elaboration, thermal stability, electrical resistance, high strength, lower creep and shrinkage, elimination, decomposition, immobilization, and encapsulation of organic and inorganic pollutants [15–18].

The term geopolymer or inorganic silicate-aluminate material was coined by Joseph Davidovits in 1979 [19]. The geopolymer matrix is an amorphous inorganic polymer elaborated using the polycondensation reaction of aluminosilicate source materials (fly ash, rice husk, metakaolin, perlite, and so on) with highly alkaline or acidic activator mediums at room temperature or with a low temperature (<100°C). This material is basically an inorganic aluminosilicate polymer consisting of recurring units, for example, poly(sialate) $(\text{-Si-O-Al-O-})_n$, poly(sialate-siloxo) $(\text{-Si-O-Al-O-Si-O-})_n$, and poly(sialate-disiloxo) $(\text{-Si-O-Al-O-Si-O-Si-O-})_n$. The structure of this amorphous material is related to the ratio of Si/Al [19]. A general chemical structure of inorganic aluminosilicate polymer could be expressed as [20]

$$M_n\left\{\left(-\mathrm{SiO_2}\right)_q - \mathrm{AlO_2}-\right\}_n, \quad (1)$$

where M denotes an alkali cation (K^+, Na^+, etc.), n represents the degree of polymerization, and q is the Si/Al ratio.

In previous studies, geopolymer matrices were elaborated by two activator mediums such as alkaline solution (K^+, Na^+, Ca^{2+}, etc.) and in acidic solution such as phosphoric acid [21, 22]. The morphological and microstructures of these new generations of mortars are evaluated by several analysis methods. The quantitative X-ray diffraction Rietveld method has been implemented to determine the quantitative chemical composition of amorphous and crystalline phases contents in the geopolymers [23]. The TGA analysis has been performed to identify the water molecules in the structure of geopolymers. The formation of the aluminosilicate hydrate gel on particle surfaces of the raw materials (fly ash, metakaolin, etc.) and its dissolution have been observed by the SEM technique [24]. The FTIR analysis has been performed to detect the new peaks related to the formation of noncrystalline aluminasilicate phase hydrate in geopolymer structures [25]. Different amorphous inorganic polymer materials developed by acidic or alkaline mediums have good mechanical properties [26], chemical properties and electrical properties [27, 28], water resistance and thermal behavior [29], and acidic and alkaline environment resistance [30]. The mechanical, thermal, durability, microstructural, and dielectric performances of inorganic polymers or geopolymers were highly influenced by the type of raw materials [31], hydroxide concentration [32], alkaline solution type [26], Si/Al [23], SiO_2/Na_2O, Al_2O_3/Na_2O ratios, maturation time [33], temperature curing [34], and so on.

Many experiments were performed to examine the impact of the type and proportion of raw materials, activator solutions, and curing conditions on the mechanical properties of geopolymer materials. For example, Louati et al. showed the mechanical strength test results of a clay-based geopolymer elaborated by illito-kaolinitic clay and phosphoric acid. In the experiments, when the liquid-to-binder ratio was set as a constant, the mechanical strength values increased with the increase in the Si-to-P molar ratio, and the mechanical strength value attains a 37 MPa when the Si/P equals 2.75 [22]. In other studies, Villaquirán-Caicedo and de Gutiérrez developed geopolymers based on commercial metakaolin and activator materials (potassium silicate and Sika Fume). The results of the mechanical strength experiment revealed that the geopolymer material activated by Sika Fume and exposed to 1200°C yielded the highest mechanical strength of 148.5 MPa [35]. Fan et al. synthesized geopolymer binders from fly ash as a raw material with KOH solution and water/fly ash ratios and obtained the geopolymer matrices with the compressive strength between 80 and 110 MPa after heating from 500°C to 800°C, respectively [36]. Therefore, these previous studies developed the concept for formulation of geopolymer binders by different aluminosilicate precursors and alkaline activators and evaluation of the physicochemical properties of these materials.

In this connection, the main aim of the present paper is to compare the impact of potassium and sodium-based activators on the morphological and compressive strength and dielectric and thermal properties of class F fly ash-based geopolymers. The effect of alkaline solutions ratio used for producing fly ash-based geopolymers has been examined by means XRD, FTIR, and SEM/EDX. The properties of the produced materials by fly ash and different alkaline activators ratios are investigated and discussed.

2. Experimental Procedures

2.1. Materials. The class F fly ash (FA) was collected from Jorf Lasfar power plant at El Jadida, Morocco, and used as a source of aluminosilicate. The chemical composition of this material as characterized by X-ray fluorescence technique is presented in Table 1.

Sodium hydroxide pellets (NaOH, 99% purity, "Sigma Aldrich," Germany), potassium hydroxide pellets (KOH, 99% purity, "Sigma Aldrich," Germany), and sodium silicate solution (Na_2SiO_3, 18% Na_2O, and 63% SiO_2, "Riedel-de-Haën," Germany) were the starting materials to prepare the alkaline activator solutions.

2.2. Preparation of Geopolymers. The alkaline media used result from the ratios between mixtures of NaOH (12M) and KOH (12M) with the sodium silicate solution (Table 2). The activator medium was mixed for 15 min to create a homogeneous mixture. To form the amorphous aluminosilicate geopolymer pastes, the fly ash is mixed with the binder liquor in a mass ratio (fly ash/alkaline solution) equal to 2.5 for 15 min using mixing machine [38, 39]. The prepared pastes were molded in a cylindrical plastic and vibrated for

Table 1: Oxide percentages of the class F fly ash [37].

Component	SiO_2	Al_2O_3	Fe_2O_3	K_2O	TiO_2	MgO	CaO	LOI
Content (%)	52.5	30.2	2.94	2.08	1.03	1.23	0.822	7.12

Table 2: Designation of the different geopolymer mixtures.

Sample code	% NaOH	% KOH	Na_2SiO_3/NaOH or KOH	Fly ash/activators
G_0	0	100		
G_1	25	75		
G_2	50	50	2.5	2.5
G_3	75	25		
G_4	100	0		

10 minutes to eliminate the gas bubbles. The geopolymer pastes were hardened at temperature 60°C for 24 hours [39]. Subsequently, all specimens were cured at ambient temperature for 28 days and then analyzed.

2.3. Analysis and Test Methods. Transmission electron microscopy (TEM) (FEI Tecnai G2) was used to obtain the fly ash morphology. The N_2 adsorption-desorption isotherms at 77 K were recorded for raw material on a Micrometrics model 3Flex 3500 instrument. The surface area of fly ash was analyzed by the Brunauer-Emmett-Teller (BET) analysis. The pore size and pore volume were calculated using the Barrett-Joyner-Halenda (BJH) method.

The structural analysis was conducted using X-ray diffraction using Cu-Ka (Xpert Pro model diffractometer). The functional group identification of all samples was undertaken by FTIR spectrophotometer (Bruker Platinum ATR).

The microstructure of the specimens was detected via scanning electron microscope coupled with energy dispersive spectroscope (SEM/EDX, JEOL-6300).

The compressive strength tests were performed by EM MODEL 00 UNIVERSAL testing machine with a 20 kN load cell according to a computer. The test was done on five cylindrical specimens (30 mm diameter and 60 mm height) with a crosshead speed of 10 mm/min at ambient temperature.

Dielectric measurements of the silver-coated pellets of the geopolymers were done as function of frequencies in the range from 20 Hz to 1 MHz at room temperature using "HP LCR Meter 4284A" at an oscillation voltage of 1 V.

Then, all specimens are heated for 2 hours at the following temperatures: 200, 400, 600, and 800°C in a programmable furnace Nabertherm.

3. Results and Discussion

3.1. Characterization of Raw Material. TEM analysis was conducted to better elucidate the morphology of fly ash (Figure 1(a)); the obtained image revealed that the fly ash consists mainly of spherical particles of different sizes. EDX spectra (Figure 1(b)) show that the raw material is composed of O (31.9%), Al (26.7%), and Si (26%) element majors.

Figures 2(a)-2(b) present the nitrogen adsorption/desorption isotherms and pore size distribution of fly ash, characterized by the BET and BJH models, respectively. The pore volume of fly ash decreased linearly with pore width increases between 1.946 and 15 nm, suggesting a heterogeneous pore size distribution in this raw material. The maximum value of pore volume at 5.10^{-5} cm^3/g corresponds to a pore size of 1.946 nm. The surface area and maximum pore volume of fly ash are presented in Table 3. The fly ash possesses a BET specific surface area of 3.5876 m^2/g and the maximum pore volume of 0.001567 cm^3/g at $p/p^\circ = 0.148548356$ and median pore width of 1.1726 nm (Horvath-Kawazoe method). The fly ash was classified as mesoporous material with average pore sizes between 2 and 50 nm, according to the IUPAC classification [40], and this material follows the type IV isotherms.

3.2. Characterization of Materials

3.2.1. XRD Analysis. The XRD patterns of fly ash and geopolymer pastes for different KOH/NaOH ratios are given in Figure 3. The fly ash consists of the crystalline phases (quartz and mullite) and a semicrystalline phase as denoted by the broad halo between 15° and 40°. In this hump, the fly ash is described by a major peak observed at $2\theta = 26.56^\circ$. When the fly ash was activated with alkaline mediums, the major peak is shifted to 26.60° for the synthesized geopolymers (G_0, G_1, and G_2) and disappeared for the other elaborated materials (G_3 and G_4). The intensity of this peak decreases with the increase of the NaOH concentration resulting in an increase in the degree of dissolution of fly ash particles [23]. Furthermore, a new peak is identified for the geopolymers G_0, G_1, and G_2 at 29.36° which shifts at 29.09° for G_3 and G_4. These peaks are commonly attributed to the alkaline alumina-silicate hydrate gel, namely, potassium/sodium-alumina-silicate hydrate gel (KASH and/or NASH) with a structure (K_2O-Al_2O_3-SiO_2-H_2O and/or Na_2O-Al_2O_3-SiO_2-H_2O), in accordance with previous findings [41, 42]. The formation of NASH and/or KASH gel can be explained by the dissolution of the fly ash particles in the different alkaline activator mediums (Na^+ and K^+). Similar findings were detailed in a previous research [43].

3.2.2. FTIR Analysis. The infrared analysis spectra of fly ash and synthesized geopolymers are displayed in Figure 4. Based on the results presented for fly ash, the band observed

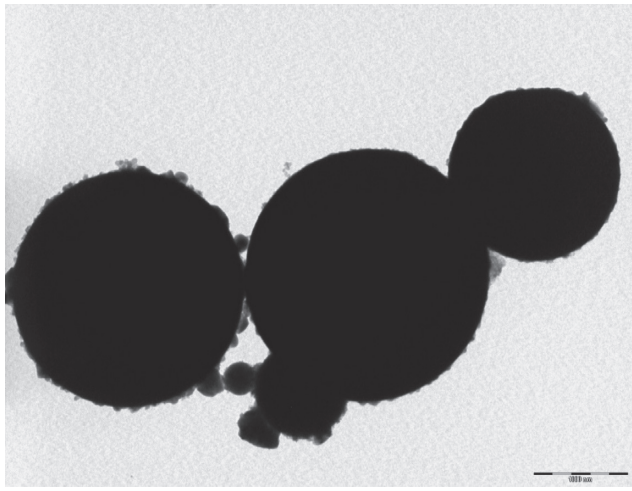

(a)

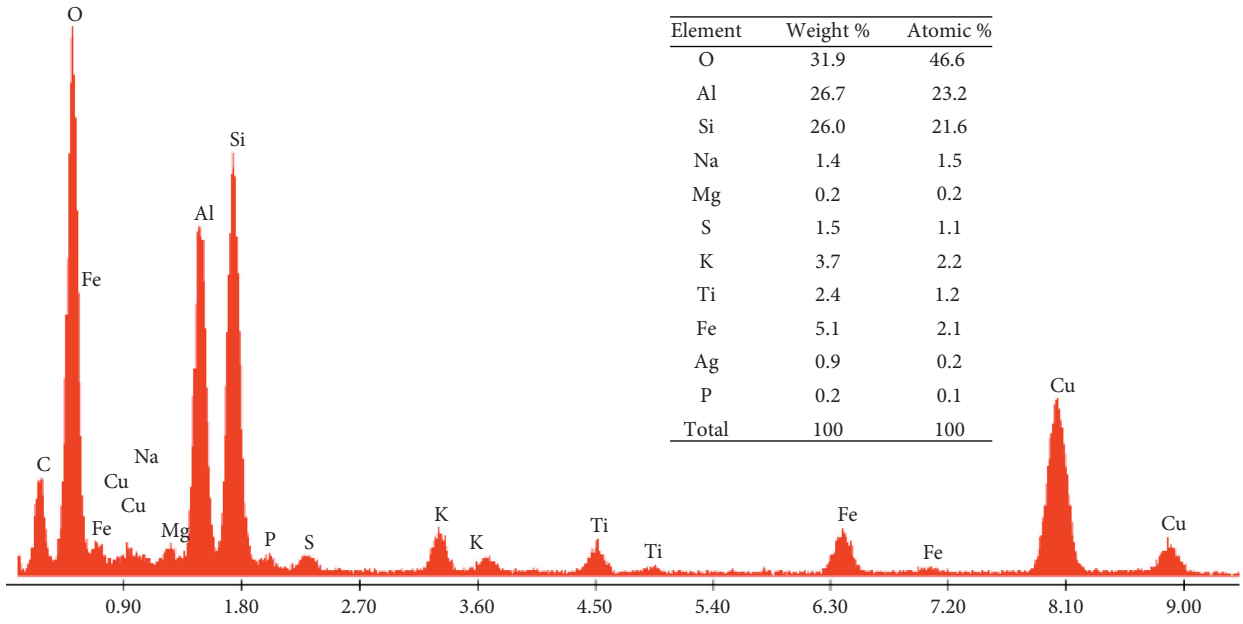

Element	Weight %	Atomic %
O	31.9	46.6
Al	26.7	23.2
Si	26.0	21.6
Na	1.4	1.5
Mg	0.2	0.2
S	1.5	1.1
K	3.7	2.2
Ti	2.4	1.2
Fe	5.1	2.1
Ag	0.9	0.2
P	0.2	0.1
Total	100	100

(b)

Figure 1: TEM image (a) and EDX (b) of fly ash.

at 1424 cm^{-1} is due to the stretching vibration of C-O. The broadband at around 1023 cm^{-1} is due to symmetric stretching vibrations of Si-O-T (T = Si or Al). The band observed at 439 cm^{-1} can be related to the stretching asymmetric vibrations of Si-O-T (T = Si or Al). The weak band arising at 874 cm^{-1} indicates the presence of semicrystalline phase in fly ash [44]. After the geopolymerization reaction, the new bands approximately about 1645 and 3365 cm^{-1} are assigned to H-O-H and O-H stretching and deformation, respectively [45]. The bands occurring in the regions of 1395 and 1439 cm^{-1} could be assigned to the asymmetric stretching vibration of CO_3^{2-}. These bands suggest the formation of sodium or potassium carbonates after geopolymerization reaction process [44]. The broad peak at 1023 cm^{-1} is due to the asymmetric stretching vibration of groups (Si-O-T, T = Si, or Al) in fly ash, which shifts to lower frequencies (954 cm^{-1}), indicating the creation of potassium/sodium alumina-silicate gel in geopolymer matrices [46, 47].

3.2.3. Microstructural Analysis. The SEM images of the F fly ash and samples formulated using different alkaline activators are depicted in Figure 5. The morphology of the fly ash is illustrated in Figure 5(a). It can be seen that this material takes the form of isolated spheres of different sizes. The smaller spheres are called microspheres that can be dense or hollow, known as "cenospheres," and several microspheres are contained in a macroparticle, known as "plerosphere," which are amorphous alumina- and/or silica-rich materials [48]. We can note that the fly ash contains crystalline phases. The data confirm the provided results by

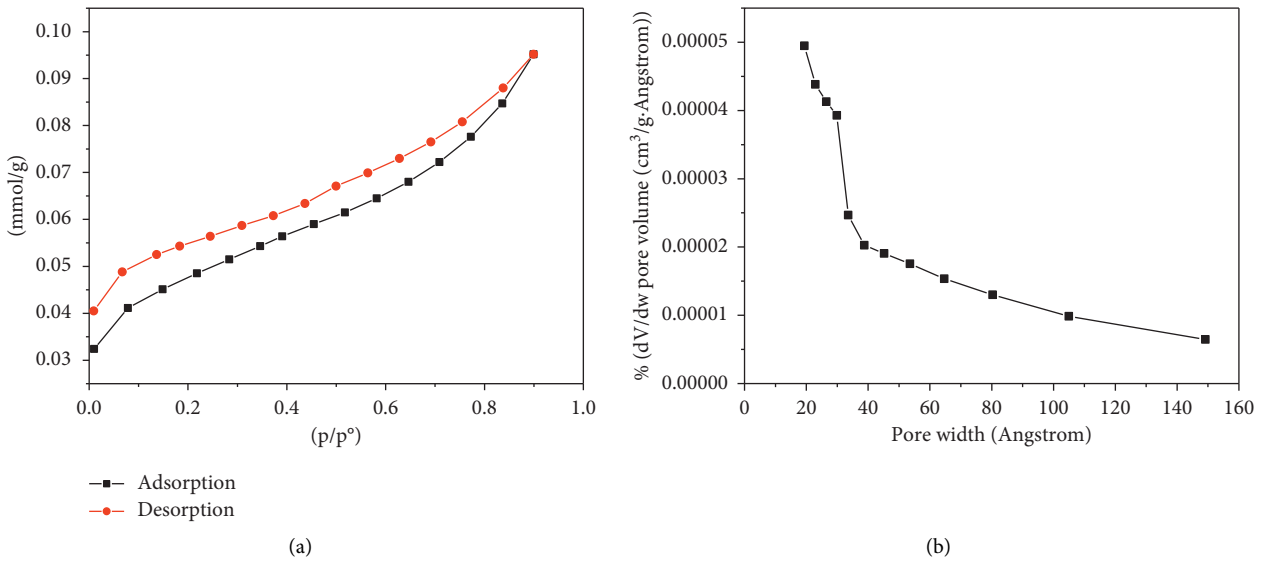

Figure 2: N_2 adsorption-desorption isotherm (a) and the pore size distribution (b) of fly ash.

Table 3: Surface area and pore properties of the fly ash.

BET surface area (m^2/g)	BJH cumulative surface area of pores (m^2/g)		Maximum pore volume (cm^3/g)
	Adsorption	Desorption	
3.5876	2.043	1.7168	0.001567

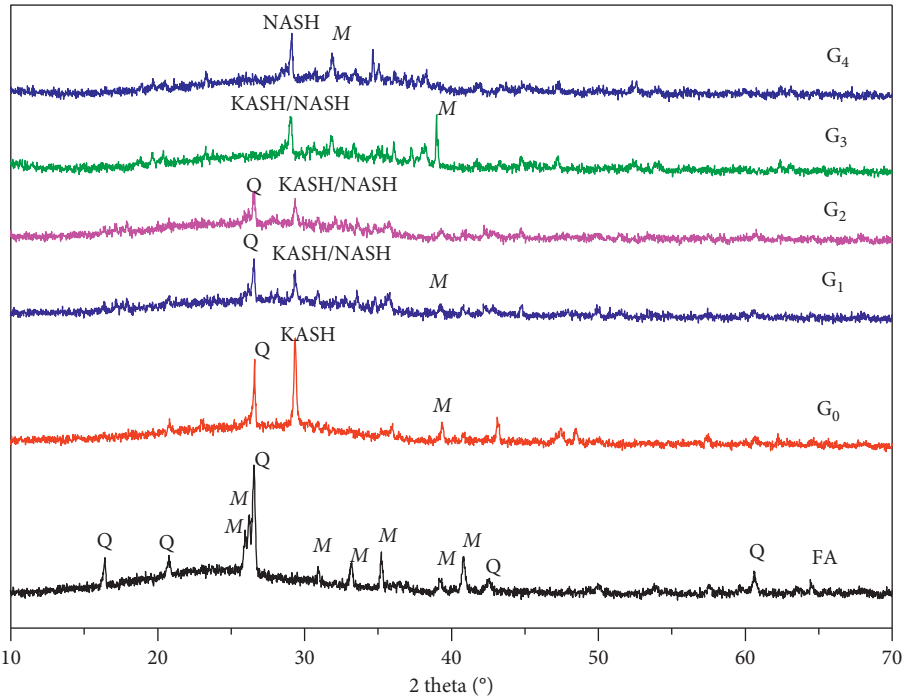

Figure 3: XRD patterns of fly ash and geopolymers dried at room temperature with different ratio of NaOH and KOH (Q: quartz; M: mullite; KASH/NASH: potassium/sodium aluminosilicate hydrate gel).

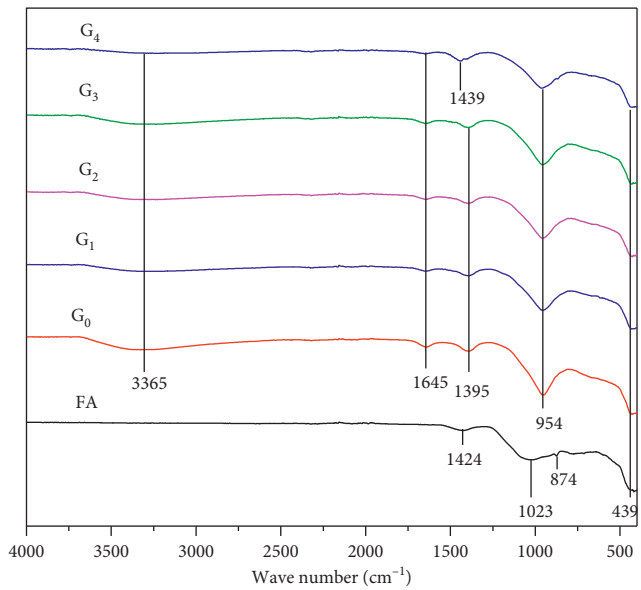

Figure 4: FTIR spectra of fly ash and geopolymer matrices cured at room temperature with different ratio of NaOH and KOH.

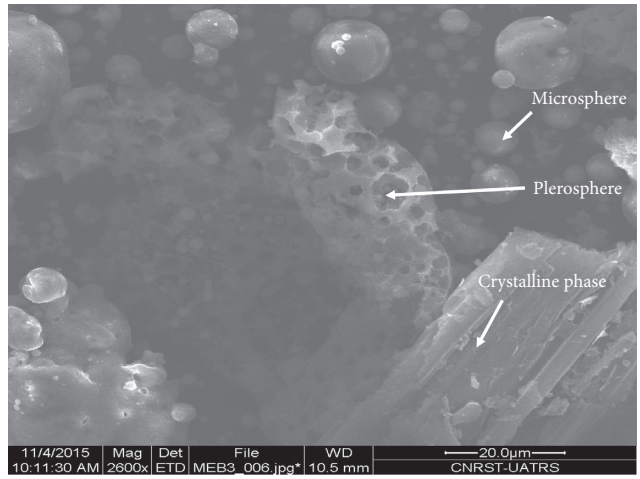

(a)

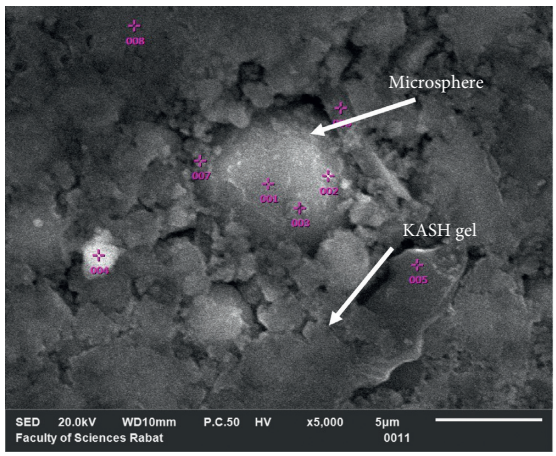

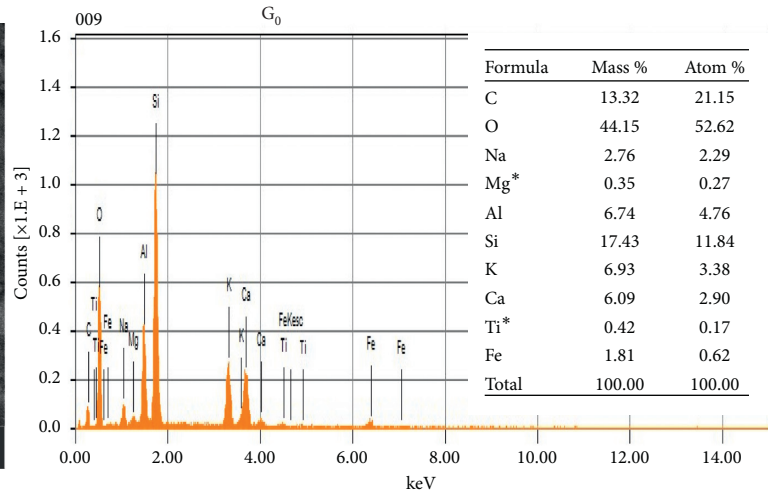

Formula	Mass %	Atom %
C	13.32	21.15
O	44.15	52.62
Na	2.76	2.29
Mg*	0.35	0.27
Al	6.74	4.76
Si	17.43	11.84
K	6.93	3.38
Ca	6.09	2.90
Ti*	0.42	0.17
Fe	1.81	0.62
Total	100.00	100.00

(b)

Figure 5: Continued.

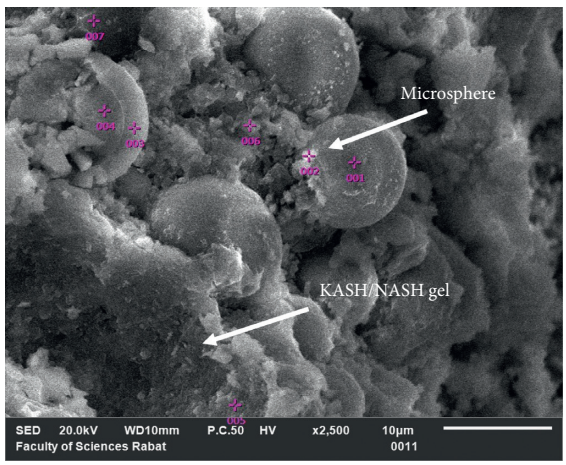

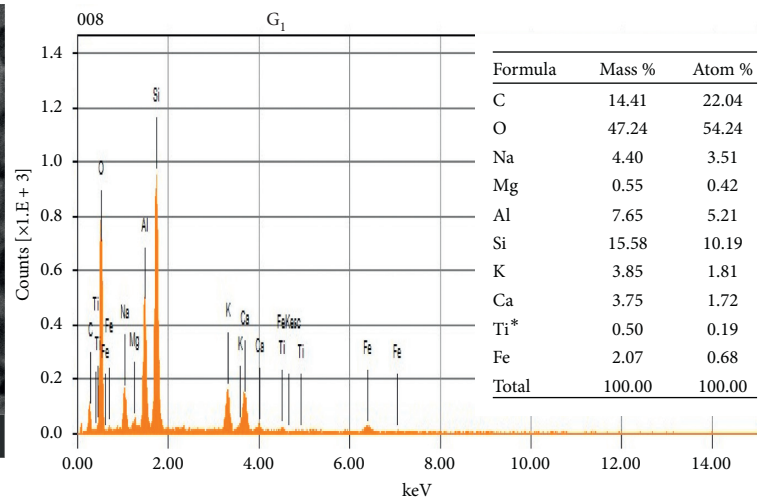

Formula	Mass %	Atom %
C	14.41	22.04
O	47.24	54.24
Na	4.40	3.51
Mg	0.55	0.42
Al	7.65	5.21
Si	15.58	10.19
K	3.85	1.81
Ca	3.75	1.72
Ti*	0.50	0.19
Fe	2.07	0.68
Total	100.00	100.00

(c)

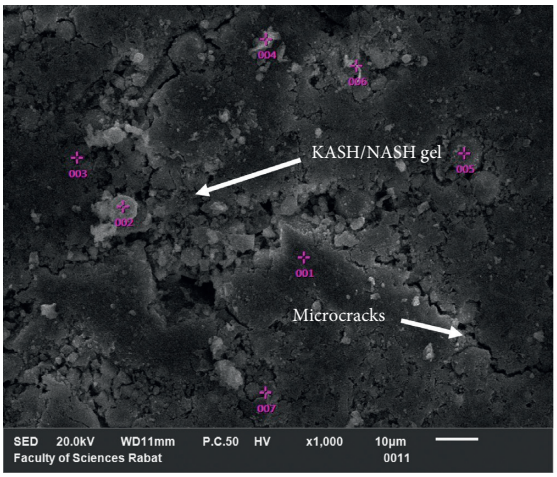

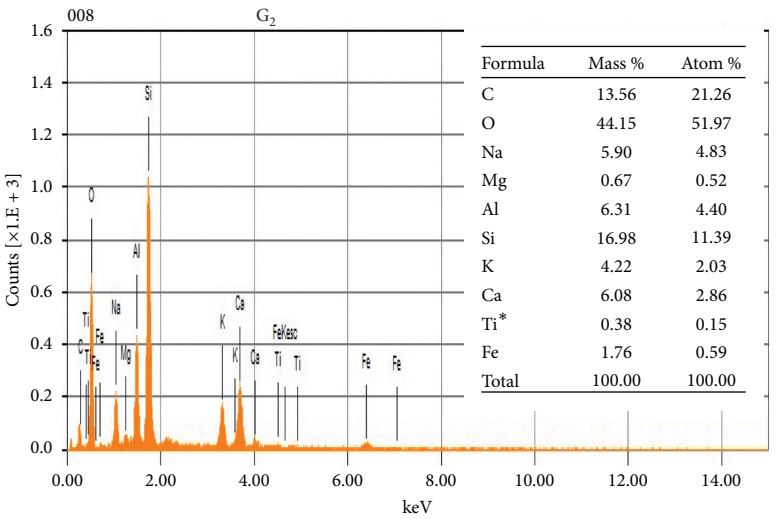

Formula	Mass %	Atom %
C	13.56	21.26
O	44.15	51.97
Na	5.90	4.83
Mg	0.67	0.52
Al	6.31	4.40
Si	16.98	11.39
K	4.22	2.03
Ca	6.08	2.86
Ti*	0.38	0.15
Fe	1.76	0.59
Total	100.00	100.00

(d)

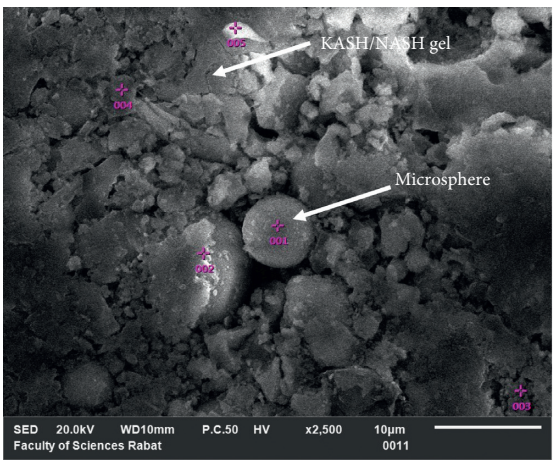

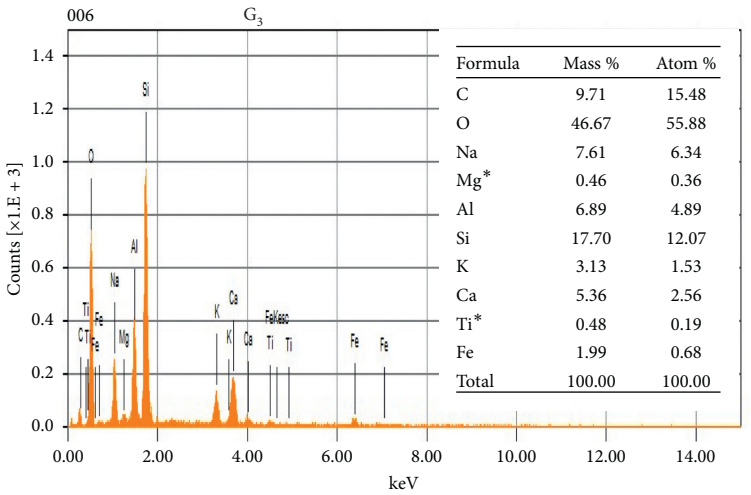

Formula	Mass %	Atom %
C	9.71	15.48
O	46.67	55.88
Na	7.61	6.34
Mg*	0.46	0.36
Al	6.89	4.89
Si	17.70	12.07
K	3.13	1.53
Ca	5.36	2.56
Ti*	0.48	0.19
Fe	1.99	0.68
Total	100.00	100.00

(e)

Figure 5: Continued.

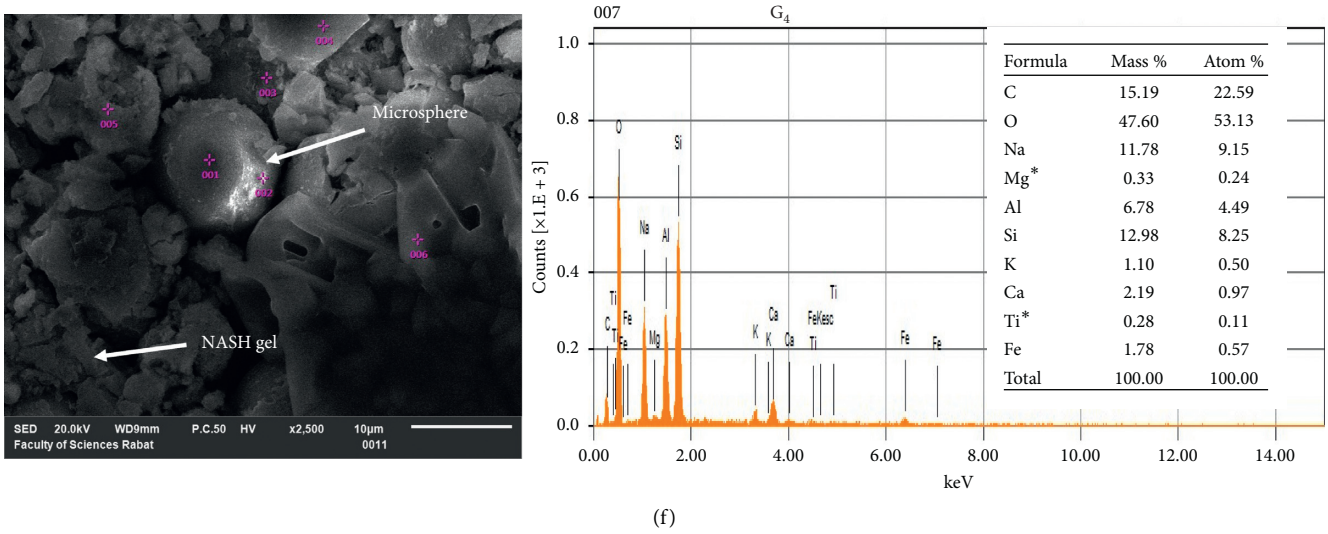

(f)

Figure 5: SEM micrographs of fly ash (a) and specimens with KOH/NaOH ratios, (b) G_0 (100% KOH), (c) G_1 (75% KOH; 25% NaOH), (d) G_2 (50% KOH; 50% NaOH), (e) G_3 (25% KOH; 75% NaOH), and (f) G_4 (100% NaOH).

XRD and FTIR analysis. According to the SEM analysis, the micrographs indicate a fundamental difference in the microstructure of the elaborated materials. These observations are interpreted by the increase of KOH content, which increases the polycondensation stage in the geopolymerization reaction.

The increase of the KOH in the system allows the increase in the formation of alumina-silicate gel on the surface of the fly ash particles. This result can be interpreted by the presence of the high amount of K^+ in the mixture, which is responsible for the high condensation rate; this promotes denser structure and strong bonding between fly ash aggregates and alkali activator medium compared to Na^+ ions [49]. The obtained data indicated that the geopolymerization process is more affected by the polycondensation step than the dissolution one.

From the EDX data, not much difference in the chemical composition was identified for the elaborated products. The main elements in the developed geopolymers are Al, Si, Na, and K. The main difference is the percentage of the elements K and Na in the microstructural of the formed materials; this difference is explained by the KOH/NaOH ratio in the formulation of specimens. The elements K and Na participate in the geopolymerization process by creating bonds in the potassium and sodium alumina-silicate gels (KASH and NASH) and form a compact structure in the amorphous inorganic polymer system [50]. SEM and EDX analysis provided the influence of Na^+ and K^+ on the structure of formed materials.

3.2.4. Mechanical Properties. Figure 6 shows the compressive strengths of geopolymer pastes formulated from fly ash and alkaline activators with different mass ratios (KOH/NaOH). Firstly, it can be observed that 100% KOH geopolymer with a value of 27 MPa has a higher compressive strength compared to 100% NaOH geopolymer

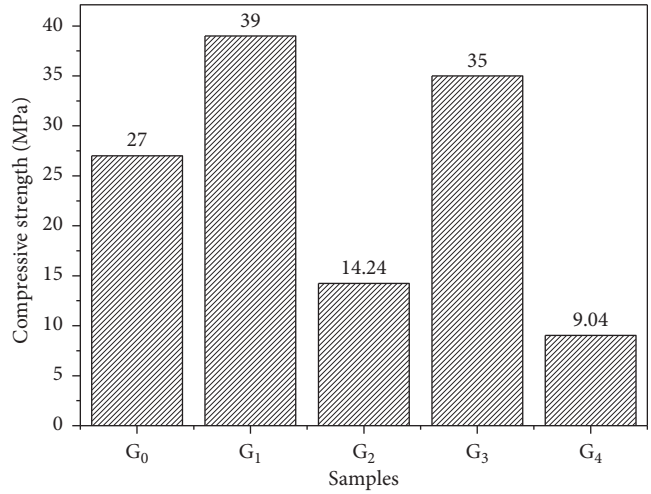

Figure 6: Compressive strength of geopolymer matrix cured at room temperature with different ratio between NaOH and KOH.

with a value of 9.04 MPa. These results were explained by physical and chemical points. Physical point: the size of metal cation K^+ (1.33 Å) is larger than that of Na^+ ion (0.97 Å); this difference leads to formation of compact structure in the geopolymer matrix. Chemical point: the metal cation K^+ should be associated with more water molecules than the metal cation Na^+; this phenomenon leads to an increase in the condensation step in the geopolymerization reaction during the formation and the creation of amorphous alumina-silicate structures. As a result, potassium-based geopolymer is more compact and denser than sodium-based geopolymer, leading to high compressive strengths [49, 51].

The obtained results, by the compressive strength tests correlating with the observations noted with microstructural SEM analysis, are in agreement with the works of Hosan

et al. [52] and Sapture et al. [53]. The authors reported that the fly ash geopolymers synthesized from KOH give a better mechanical performance in terms of resistance to compression. We can see that the geopolymer elaborated with 75% KOH/25% NaOH has the highest compressive strength with a value of 39 MPa followed by 25% KOH/75% NaOH geopolymer with a value of 35 MPa. These compressive strengths are greater than the 100% KOH geopolymer (27 MPa), 50% KOH/50% NaOH geopolymer (14.24 MPa), and 100% NaOH geopolymer (9.04 MPa). The obtained values can be explained by the synergistic effect between Na^+, which allows good dissolution of the raw material, and the formation of more monomer entities and the potassium ions, which favors the formation of oligomers by polycondensation. The aluminosilicate gel is formed around the nonpartially or partially solubilized fly ash particles. The geopolymer G_2 shows a low compressive strength compared to G_1 and G_3.

The obtained results were confirmed by SEM and XRD analysis (due to the partial formation of an aluminosilicate gel on the raw material particles and the formation of microcracks in the G_2 material). These observations were elucidated by the kinetics of each step (dissolution, restriction, and polycondensation) of the physicochemical reactions of the aggregate particles and the ratio of the activating solutions to the geopolymerization process. The good formation of alumina-silicate gel on the fly ash surface leads to the compact structure of the geopolymers. The three stages of the geopolymerization reaction are favored, inducing the formation of geopolymers with high compressive strengths [54]. The results of compressive strength tests indicate that the decrease or increase of compressive strength of the formulated geopolymers is highly dependent on the cation type (Na^+ and K^+) and mixing ratio KOH/NaOH.

Table 4 summarizes the compressive strength values of geopolymers formulated from different solid precursors. The comparison of the compressive strengths of different geopolymers shows that the fly ash-based geopolymers have higher compressive strengths than the geopolymers developed by other materials. Therefore, these results suggest that the elaborated materials are more suitable for construction applications. In addition, the best resistance is achieved with class F fly ash, which is among the best precursors rich in aluminosilicate for the development of geopolymer binders.

3.2.5. Dielectric Properties. The variation of dielectric permittivity with frequency for fly ash-based geopolymer pastes is shown in Figure 7. According to the data, dielectric permittivity decreased for geopolymers with the increase in the frequencies. This suggests a dispersion region resulting from the relaxation of the polarization process in the system [58]. At low frequencies, the dielectric permittivity decreases with the decrease in KOH mass in the KOH/NaOH ratio of the elaborated materials. At high frequencies, the dielectric permittivity continues to decrease before becoming almost constant in the high frequency's region, which could be the result of the decrease in the number of free charges provided by NaOH, KOH, and H_2O in the geopolymeric pastes. The dielectric permittivity of the developed geopolymers has been improved by the ion polarization process provided by potassium hydroxide, sodium hydroxide, and ionized water. It can be seen that the dielectric properties of the elaborated specimens are monitored by the ionic conductivity provided by the K^+ and Na^+ ions.

Table 4: Comparison of the compressive strength of material-based geopolymer mortars.

Geopolymer-based materials	Compressive strength of geopolymer (MPa)	References
Sewage sludge and metakaolin-based geopolymer	50	[55]
Metakaolin-based geopolymer	29	[56]
Ceramic dust waste-based geopolymer bricks	9	[57]
Phosphate-based geopolymer	29.9	[15]
Clay-based geopolymer	36	[32]
Fly ash-based geopolymer	39	This study

3.2.6. Thermal Test. The prepared geopolymers were cured at ambient temperature up to 28 days and then treated in the range of 200 and 800°C for 2 hours. Figure 8 displays the specimens before and after the heat treatment. After exposure to high temperatures, the color of the geopolymers becomes lighter and beige due to the evaporation of the water molecules that exist in the structure of the matrix. The geopolymers formed by several activators are well preserved after heating at 400°C and show no surface cracking. After annealing at 600°C, the KOH-activated geopolymer is well preserved after heating and shows no surface cracking. At 800°C, small cracks are observed in the specimen elaborated by KOH and the cracks increase when the percentage of NaOH increases in the geopolymers. These results were due to the degree of polycondensation of the fly ash particles in different alkaline solutions. Indeed, the increase of the mass ratio KOH/NaOH in the alkaline solution favors the polycondensation caused by the large solubilization of fly ash particles. This observation can be interpreted by the fact that K^+ ions are responsible for a higher degree of condensation rate, thus more effectively promoting the polycondensation step to obtain a more compact and more heat-resistant product compared to Na^+ ions [49]. This corroborates the result obtained by the SEM analysis, which suggests that the degree of alumina-silicate hydrate gel formation in the potassium hydroxide-based geopolymer is higher than in those synthesized from sodium hydroxide. Similar findings have been reported by Rocha et al. [59] and Hosan et al. [60]. These results proved that the investigated geopolymer matrices represent a potential candidate for fire protection and safety engineering technology.

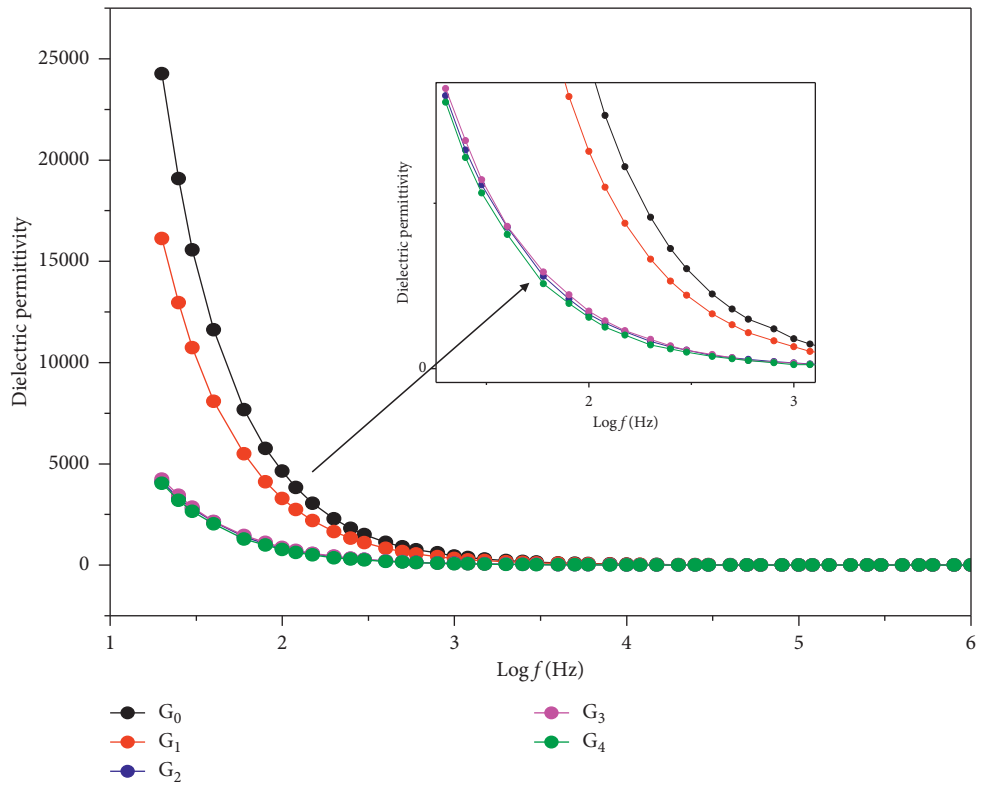

Figure 7: Real part of dielectric permittivity of geopolymer matrices cured at room temperature with different ratio between NaOH and KOH.

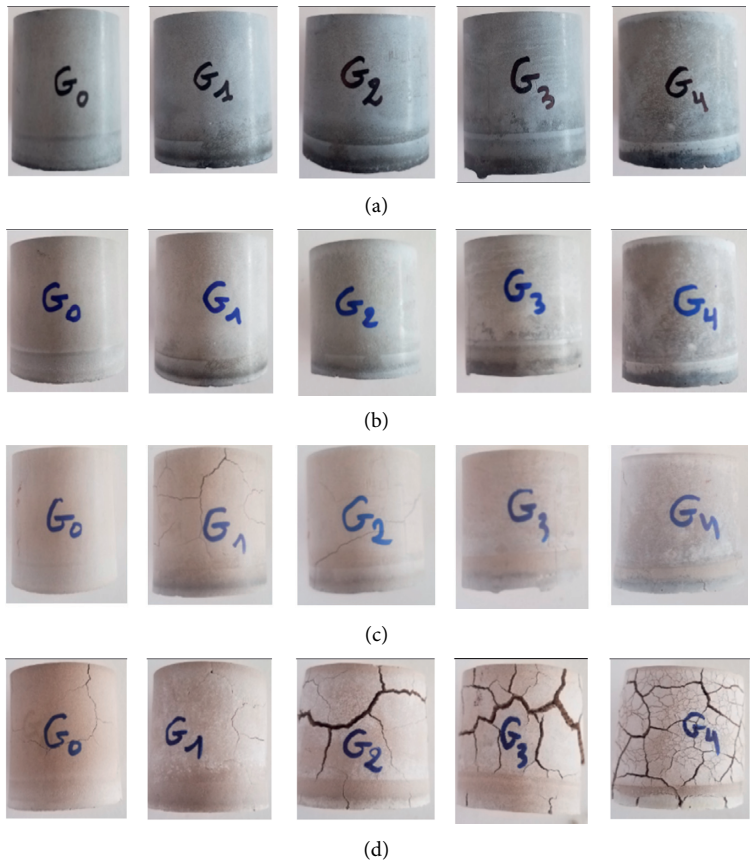

Figure 8: The photographs of geopolymers specimens cared for at different temperatures. (a) 200°C. (b) 400°C. (c) 600°C. (d) 800°C.

4. Conclusions

In this research, the influence of different alkali solutions (Na^+ and K^+) on the physicochemical properties of the geopolymers was examined. The experimental findings of this research are summarized as follows:

(i) The FTIR and XRD analysis uncovered the development of an alkali (Na^+/K^+) alumina-silicate hydrate gel in the surface of the obtained geopolymers.

(ii) The SEM analysis validated the creation of the alumina-silicate gel by dissolving the fly ash particles in the alkaline mediums, and the polycondensation step depends on the type of alkaline activator media.

(iii) The compressive strength of all specimens with different ratios between KOH and NaOH was examined. It was found that a yield between 9.04 and 39 MPa and the maximum compressive strength were achieved when the ratio of KOH/NaOH was 75%/25% with compressive strength 39 MPa.

(iv) The geopolymer prepared with NaOH is characterized by low dielectric parameters, suggesting that it is suitable to be used in electrical insulation. The specimen based on fly ash and KOH is more thermally stable.

The obtained results confirm that the type of alkali activator medium used has a significant influence on the morphological, structural, mechanical, electrical, and thermal properties of the formed geopolymer binders. These results encourage the use of fly ash (waste) as an aluminosilicate-rich material to create aluminosilicate geopolymer. These geopolymers can be used in various fields such as construction applications, electrical insulation, and building fire protection.

Data Availability

All the data are included in the manuscript.

Conflicts of Interest

The authors declare that they have no conflicts of interest.

References

[1] S. A. Miller, A. Horvath, and P. J. M. Monteiro, "Readily implementable techniques can cut annual CO_2 emissions from the production of concrete by over 20%," *Environmental Research Letters*, vol. 11, no. 7, Article ID 074029, 2016.

[2] C.-Y. Zhang, R. Han, B. Yu, and Y.-M. Wei, "Accounting process-related CO_2 emissions from global cement production under Shared Socioeconomic Pathways," *Journal of Cleaner Production*, vol. 184, pp. 451–465, 2018.

[3] G. Habert, "Assessing the environmental impact of conventional and "green" cement production," in *Eco-Efficient Construction and Building Materials*, pp. 199–238, Elsevier, Amsterdam, Netherlands, 2014.

[4] M. B. Ali, R. Saidur, and M. S. Hossain, "A review on emission analysis in cement industries," *Renewable and Sustainable Energy Reviews*, vol. 15, no. 5, pp. 2252–2261, 2011.

[5] J. S. J. Deja, J. L. Uliasz-Bochenczyk, and E. Mokrzycki, "CO_2 emissions from Polish cement industry," *Waste and Biomass Valorization*, vol. 4, no. 1, pp. 583–588, 2010.

[6] N. B. Assi, K. Carter, E. Deaver, R. Anay, and P. Ziehl, "Sustainable concrete: building a greener future," *Journal of Cleaner Production*, vol. 198, pp. 1641–1651, 2018.

[7] B. Nematollahi, J. Sanjayan, and F. U. A. Shaikh, "Synthesis of heat and ambient cured one-part geopolymer mixes with different grades of sodium silicate," *Ceramics International*, vol. 41, pp. 5696–5704, 2015.

[8] J. S. J. van Deventer, J. L. Provis, P. Duxson, and D. G. Brice, "Chemical research and climate change as drivers in the commercial adoption of alkali activated materials," *Waste and Biomass Valorization*, vol. 1, no. 1, pp. 145–155, 2010.

[9] N. B. Singh, M. Kumar, and S. Rai, "Geopolymer cement and concrete: Properties," *Materials Today: Proceedings*, vol. 29, pp. 743–748, 2020.

[10] A. Mehta and K. K. Siddique, "Properties of low-calcium fly ash based geopolymer concrete incorporating OPC as partial replacement of fly ash," *Materials & Design*, vol. 150, pp. 792–807, 2017.

[11] X. Jiang, J. Y. Zhang, R. Xiao et al., "A comparative study on geopolymers synthesized by different classes of fly ash after exposure to elevated temperatures," *Journal of Cleaner Production*, vol. 270, Article ID 122500, 2020.

[12] I. Farina, M. Modano, G. Zuccaro, R. Goodall, and F. Colangelo, "Improving flexural strength and toughness of geopolymer mortars through additively manufactured metallic rebars," *Composites Part B: Engineering*, vol. 145, pp. 155–161, 2018.

[13] M. Lahoti, K. K. Wong, K. H. Tan, and E.-H. Yang, "Effect of alkali cation type on strength endurance of fly ash geopolymers subject to high temperature exposure," *Materials & Design*, vol. 154, pp. 8–19, 2018.

[14] A. Martin, J. Y. Pastor, A. Palomo, and M. H. Fernández Jiménez, "Mechanical behaviour at high temperature of alkali-activated aluminosilicates (geopolymers)," *Construction and Building Materials*, vol. 93, pp. 1188–1196, 2015.

[15] M. Zribi, B. Samet, and S. Baklouti, "Effect of curing temperature on the synthesis, structure and mechanical properties of phosphate-based geopolymers," *Journal of Non-crystalline Solids*, vol. 511, pp. 62–67, 2019.

[16] I. Kusak, M. Lunak, and P. Rovnanik, "Electric conductivity changes in geopolymer samples with added carbon nanotubes," *Procedia Engineering*, vol. 151, pp. 157–161, 2016.

[17] N. Asim, M. Alghoul, M. Mohammad et al., "Emerging sustainable solutions for depollution: Geopolymers," *Construction and Building Materials*, vol. 199, pp. 540–548, 2019.

[18] H. K. Yousefi Oderji, C. H. Chen, M. R. Ahmad, and S. F. A. Shah, "Fresh and hardened properties of one-part fly ash-based geopolymer binders cured at room temperature: effect of slag and alkali activators," *Journal of Cleaner Production*, vol. 225, pp. 1–10, 2019.

[19] D. J. Davidovits, "30 years of successes and failures in geopolymer applications," in *Proceedings of the Market Trends and Potential Breakthroughs, Geopolymer 2002 Conference*, Melbourne, Australia, October 2002.

[20] Z. Liu, C. S. Cai, F. Liu, and F. Fan, "Feasibility study of loess stabilization with fly ash–based geopolymer," *Journal of Materials in Civil Engineering*, vol. 28, no. 5, Article ID 04016003, 2016.

[21] H. K. Tchakouté, C. H. Rüscher, E. Kamseu, F. Andreola, and C. Leonelli, "Influence of the molar concentration of phosphoric acid solution on the properties of metakaolin-phosphate-based geopolymer cements," *Applied Clay Science*, vol. 147, pp. 184–194, 2017.

[22] S. Louati, S. Baklouti, and B. Samet, "Geopolymers based on phosphoric acid and illito-kaolinitic clay," *Advances in Materials Science and Engineering*, vol. 2016, Article ID 2359759, 7 pages, 2016.

[23] R. H. Lee, G. Kim, R. Kim, B. Cho, S. Lee, and C.-M. Chon, "Strength development properties of geopolymer paste and mortar with respect to amorphous Si/Al ratio of fly ash," *Construction and Building Materials*, vol. 151, pp. 512–519, 2017.

[24] A. B. Alouani, S. Alehyen, B. E. Achouri, and M. Taibi, "Comparative studies on removal of textile dye onto geopolymeric adsorbents," *EnvironmentAsia*, vol. 12, pp. 143–153, 2019.

[25] H. K. Bagheri, C. H. Nazari, A. Hajimohammadi et al., "Microstructural study of environmentally friendly boroaluminosilicate geopolymers," *Journal of Cleaner Production*, vol. 189, pp. 805–812, 2018.

[26] R. H. Abdul Rahim, H. K. Rahmiati, K. A. Azizli, C. H. Man, M. F. Nuruddin, and L. Ismail, "Comparison of using NaOH and KOH activated fly ash-based geopolymer on the mechanical properties," *Materials Science Forum*, vol. 803, no. 3, pp. 179–184, 2014.

[27] A. B. Malkawi, H. Al-Mattarneh, B. E. Achara, B. S. Mohammed, and M. F. Nuruddin, "Dielectric properties for characterization of fly ash-based geopolymer binders," *Construction and Building Materials*, vol. 189, pp. 19–32, 2018.

[28] F. N. Tchakouté and C. H. Rüscher, "Mechanical and microstructural properties of metakaolin-based geopolymer cements from sodium waterglass and phosphoric acid solution as hardeners: a comparative study," *Applied Clay Science*, vol. 140, pp. 81–87, 2017.

[29] C. Nobouassia Bewa, H. K. Tchakouté, D. Fotio, C. H. Rüscher, E. Kamseu, and C. Leonelli, "Water resistance and thermal behavior of metakaolin-phosphate-based geopolymer cements," *Journal of Asian Ceramic Societies*, vol. 6, no. 2-3, pp. 271–283, 2018.

[30] G. S. Jin, Y. B. Zheng, K. T. Sun, Y. S. Chen, and Z. Jin, "Resistance of metakaolin-MSWI fly ash based geopolymer to acid and alkaline environments," *Journal of Non-crystalline Solids*, vol. 450, pp. 116–122, 2016.

[31] Y. J. Okoye, J. Durgaprasad, and N. B. Singh, "Fly ash/Kaolin based geopolymer green concretes and their mechanical properties," *Data in Brief*, vol. 5, no. 6, pp. 739–744, 2015.

[32] M. A. Hamdi, R. M. Ben Messaoud, and E. Srasra, "Production of geopolymer binders using clay minerals and industrial wastes," *Comptes Rendus Chimie*, vol. 22, pp. 220–226, 2019.

[33] G. S. Ryu, Y. B. Lee, K. T. Koh, and Y. S. Chung, "The mechanical properties of fly ash-based geopolymer concrete with alkaline activators," *Construction and Building Materials*, vol. 47, pp. 409–418, 2013.

[34] Y. J. Patel and N. Shah, "Removal of cationic dye—methylene blue—from aque ous solution by adsorption on fly ash—based geopolymer," *Journal of Materials and Environmental Sciences*, vol. 28, no. 1, pp. 412–421, 2018.

[35] M. A. Villaquirán-Caicedo and R. M. de Gutiérrez, "Synthesis of ceramic materials from ecofriendly geopolymer precursors," *Materials Letters*, vol. 230, pp. 300–304, 2018.

[36] F. Fan, Z. Liu, G. Xu, M. h. Peng, and C. S. Cai, "Mechanical and thermal properties of fly ash based geopolymers," *Construction and Building Materials*, vol. 2019, pp. 66–81, 2018.

[37] K. A. EL Alouani, S. Alehyen, M. EL Achouri, and M. Taibi, "Removal of cationic dye–methylene blue—from aque ous solution by adsorption on fly ash—based geopolymer," *Journal of Materials and Environmental Sciences*, vol. 9, no. 4, pp. 32–46, 2018.

[38] M. El Alouani, S. Alehyen, M. El Achouri, and M. Taibi, "Adsorption of cationic dye onto fly ash-based geopolymer: batch and fixed bed column studies," *MATEC Web of Conferences*, vol. 149, Article ID 02088, 2018.

[39] M. El Alouani, S. Alehyen, M. El Achouri et al., "Preparation, characterization, and application of metakaolin-based geopolymer for removal of methylene blue from aqueous solution," *Journal of Chemistry*, vol. 2019, Article ID 4212901, 14 pages, 2019.

[40] K. A. Cychosz and M. Thommes, "Enhanced dielectric performance of metakaolin-H_3PO_4 geopolymers," *Engineering*, vol. 4, pp. 559–566, 2018.

[41] A. B. Pascual, A. Tagnit-Hamou, A. Yahia et al., *Élaboration De Nouveaux Liants Mineraux Pour La Formulation De Bétons Ecologiques Et Durables*, University of Sherbrooke, Sherbrooke, Canada, 2014.

[42] R. Zhao, Y. Yuan, Z. Cheng et al., "Freeze-thaw resistance of Class F fly ash-based geopolymer concrete," *Construction and Building Materials*, vol. 222, no. 6, pp. 474–483, 2019.

[43] S. M. A. Douiri, F. A. Louati, S. Baklouti, M. Arous, and Z. Fakhfakh, "Enhanced dielectric performance of metakaolin–H_3PO_4 geopolymers," *Materials Letters*, vol. 164, pp. 299–302, 2016.

[44] W. K. W. Rożek, J. S. J. Król, and W. Mozgawa, "Spectroscopic studies of fly ash-based geopolymers," *Spectrochimica Acta Part A: Molecular and Biomolecular Spectroscopy*, vol. 198, no. 2-3, pp. 283–289, 2018.

[45] T. Bakharev, "Geopolymeric materials prepared using Class F fly ash and elevated temperature curing," *Cement and Concrete Research*, vol. 35, pp. 1224–1232, 2005.

[46] S. M. A. El-Gamal and F. A. Selim, "Utilization of some industrial wastes for eco-friendly cement production," *Sustainable Materials and Technologies*, vol. 12, no. 6, pp. 9–17, 2017.

[47] W. K. W. Lee and J. S. J. van Deventer, "The effects of inorganic salt contamination on the strength and durability of geopolymers," *Colloids and Surfaces A: Physicochemical and Engineering Aspects*, vol. 211, pp. 115–126, 2002.

[48] J. G. S. Choo, J. S. J. Lim, W. Lee, and C. Lee, "Compressive strength of one-part alkali activated fly ash using red mud as alkali supplier," *Industrial & Engineering Chemistry Research*, vol. 125, no. 10, pp. 21–28, 2016.

[49] M. Cyr, R. Idir, and T. Poinot, "Properties of inorganic polymer (geopolymer) mortars made of glass cullet," *Journal of Materials Science*, vol. 47, pp. 2782–2797, 2012.

[50] A. Mehta and R. Siddique, "Sulfuric acid resistance of fly ash based geopolymer concrete," *Construction and Building Materials*, vol. 146, pp. 136–143, 2017.

[51] O. M. van Jaarsveld and J. S. J. van Deventer, "Effect of the alkali metal activator on the properties of fly ash-based geopolymers," *Industrial & Engineering Chemistry Research*, vol. 38, no. 6, pp. 3932–3941, 1999.

[52] D. B. Hosan, S. Haque, and J. L. Shaikh, "Comparative study of sodium and potassium based fly ash geopolymer at elevated temperatures," in *Proceedings of the Second International Conference on Performance-Based and Life-Cycle Structural*

Engineering (PLSE 2015), pp. 1085–1092, School of Civil Engineering, The University of Queensland, Brisbane, Australia, December 2015.

[53] S. Satpute, M. Shirasath, and S. Hake, "Investigation of alkaline activators for fly-ash based geo- polymer concrete," *International Journal of Advance Research and Innovative Ideas in Education*, vol. 2, no. 5, pp. 2395–4396, 2016.

[54] O. M. Damilola, "Syntheses, characterization and binding strength of geopolymers: a review," *International Journal of Materials Science and Applications*, vol. 2, p. 185, 2013.

[55] W. J. Istuque, T. M. Soriano, J. L. Akasaki et al., "Effect of sewage sludge ash on mechanical and microstructural properties of geopolymers based on metakaolin," *Construction and Building Materials*, vol. 203, no. 2, pp. 95–103, 2019.

[56] N. Belmokhtar, H. El Ayadi, M. Ammari, and L. Ben Allal, "Effect of structural and textural properties of a ceramic industrial sludge and kaolin on the hardened geopolymer properties," *Applied Clay Science*, vol. 162, pp. 1–9, 2018.

[57] S. K. Amin, S. A. El–Sherbiny, A. A. M. A. El–Magd, A. Belal, and M. F. Abadir, "Fabrication of geopolymer bricks using ceramic dust waste," *Construction and Building Materials*, vol. 157, pp. 610–620, 2017.

[58] W. J. McCarter, T. M. Chrisp, G. Starrs, and J. Blewett, "Characterization and monitoring of cement-based systems using intrinsic electrical property measurements," *Cement and Concrete Research*, vol. 33, pp. 197–206, 2003.

[59] T. d. S. Rocha, D. P. Dias, F. C. C. França, R. R. d. S. Guerra, and L. R. d. C. d. O. Marques, "Metakaolin-based geopolymer mortars with different alkaline activators (Na^+ and K^+)," *Construction and Building Materials*, vol. 178, pp. 453–461, 2018.

[60] A. Hosan, S. Haque, and F. Shaikh, "Compressive behaviour of sodium and potassium activators synthetized fly ash geopolymer at elevated temperatures: a comparative study," *Journal of Building Engineering*, vol. 8, pp. 123–130, 2016.